Studies of a
Liquid Argon Time Projection Chamber
in a Magnetic Field

Changguo Lu and Kirk T. McDonald[1]

Joseph Henry Laboratories, Princeton University, Princeton, NJ 08544

(October 30, 2001)

Abstract

The recent dramatic success of the ICARUS 300-ton liquid-argon time-projection-chamber prototype [1] indicates that it is timely to review the possibilities for large-scale application of this technology for accelerator-based neutrino physics, neutrino astrophysics, and proton decay [2]. A full exploration of the MNS neutrino mixing matrix (and extensions if sterile neutrinos exist) should be possible if the large mixing angle MSW solution to the solar neutrino problem presently favored by the data [3] is confirmed by futures measurements. A large detector for this purpose should be able to distinguish the charge of the lepton into which the neutrino converts, for which the detector should be immersed in a magnetic field.

The most promising option for a large detector that can distinguish the charge of an electron is magnetized liquid argon [4, 5]. However, all studies to date of liquid argon detectors suitable for neutrino physics [6]-[17] have been in zero magnetic field. We propose to study two key issues for a large magnetized liquid argon detector:

1. Verification that a liquid argon detector can be operated with the electric field perpendicular to the magnetic field (unlike gas phase time projection chambers that must be operated with **E** parallel to **B**).

2. Verification that a liquid argon detector can be operated at several atmospheres pressure, as would occur near the bottom of a very large detector.

These studies are to be performed with a small detector, similar to that used to measure the electron lifetime in liquid argon [9, 10, 11, 18]. The requested funds for this are $30k.

This study will be followed by a larger (by at least an order of magnitude) effort to demonstrate the accuracy of electron charge determination as a function of electron energy in a beam test [19].

---

[1]Corresponding author: kirkmcd@princeton.edu

1 Concept of a Large Magnetized Liquid Argon Detector

The authors' interest in large detectors for neutrino physics arises from our involvement in studies for high-performance neutrino factories based on muon storage rings [20], and for neutrino superbeams from pion decay [21]. A new accelerator-based neutrino physics program must provide significant contrast to the program developing in Japan in association with the JHF [22]. The Japanese detector is the 50-kton (22-kton fiducial volume) water Čerenkov detector, Superkamiokande, presently operating with no magnetic field, with a possible upgrade to a 1-Mton detector in the future.

A superior detector must offer greater information about the neutrino interactions, particularly the sign of the leptons into which the neutrino converts, which implies that it must be immersed in a magnetic field. A water Čerenkov detector with PMT readout is not very compatible with magnetic analysis. A magnetized-iron sampling calorimeter can analyze the momentum of final state muons, but has little ability to analyze the momentum of electrons. Among devices that could be scaled to very large volumes, a magnetized liquid argon detector is the only one that can analyze electron charge (up to a few GeV), and provides the most detailed tracking information for neutrino interactions.

1- TOP END CAP IRON YOKE
2- BOTTOM END CAP IRON YOKE
3- BARREL IRON RETURN YOKE
4- COIL
5- CRYOSTAT
6- CATHODES (N° 5)
7- WIRE CHAMBERS (N° 4)
8- FIELD SHAPING ELECTRODES

LANNDD
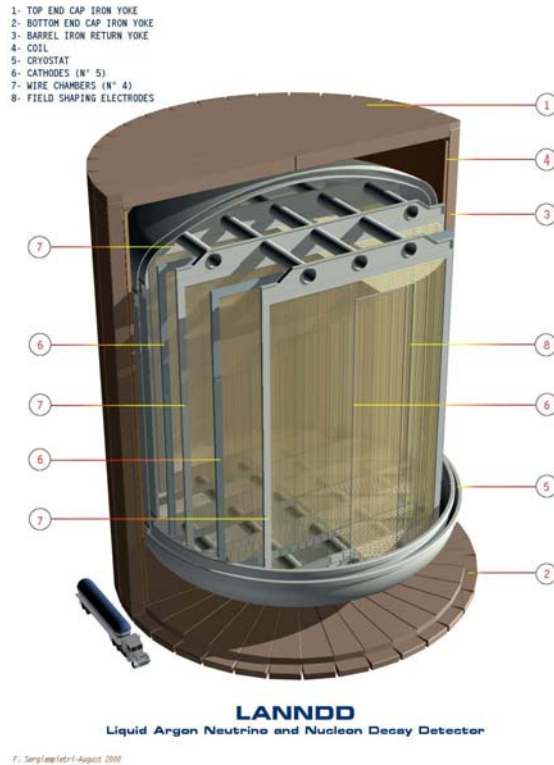Liquid Argon Neutrino and Nucleon Decay Detector

Figure 1: Concept of a 70-kton Liquid Argon Neutrino and Nucleon Decay Detector (LANNDD) [2, 5].

An overall concept of a large magnetized liquid argon detector is shown in Fig. 1. The

LANNDD is a time projection chamber, meaning that electrons ionized by charged particles from a neutrino (or other) interaction are drifted by an electric field to an x-y readout plane that is sampled in time to provide the z coordinate of pattern of ionization. Anticipating the possibility that neutrino beams are eventually sent to it from more than one accelerator, the magnetic field is vertical so the trajectories of secondary particles are generally orthogonal to the magnetic field.

1.1 Operation with E ⊥ B

To keep the readout channel count reasonably small ($\approx 200,000$), a pixel readout is not used, but rather arrays of wires at 0° and 90° to the vertical detect direct and induced signals from drifting electrons. The mechanics of the very large wire planes are somewhat easier if the planes are vertical, as shown in Fig. 1, which implies that the drift electric field is horizontal, *i.e.*, perpendicular to the magnetic field.

Furthermore, the use of crossed wire planes for the readout rather than pixels makes pattern recognition considerably easier if the electron drift is perpendicular, rather than parallel, to the magnetic field. Then, electrons from different regions of a track generally arrive at the readout plane at different times, and the problem of "ghost hits" is reduced [5, 19].
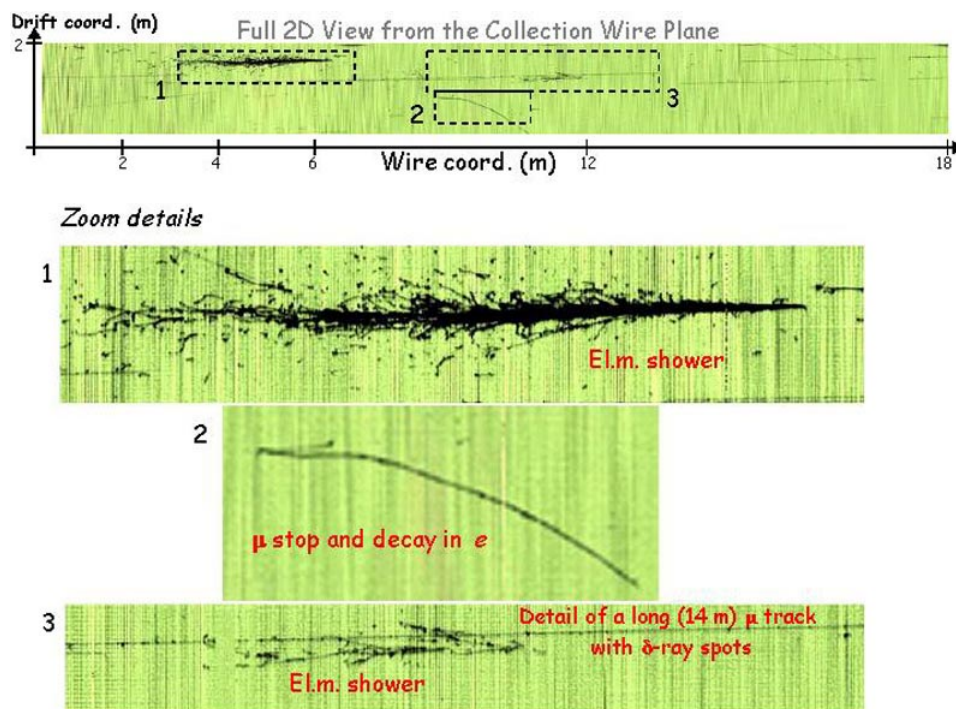

Figure 2: An event from the recent cosmic-ray test run of ICARUS [1], showing excellent track resolution over long drift distances in zero magnetic field.

All time projection chambers operated in a magnetic field to date have used a gas as the ionization medium, and have had the electric field parallel to the magnetic field. There are

two reasons for this, neither of which holds for a liquid medium. First, to obtain good momentum measurements in a gas, the electron diffusion in the bend plane must be suppressed, which requires $\mathbf{E} \parallel \mathbf{B}$. But, diffusion is so greatly suppressed in a liquid that good spatial resolution is maintained over large drift distances even in zero magnetic field, as shown in Fig. 2 from ICARUS. Second, the relatively high drift velocity of ionization electrons in a gas would result in a large "Lorentz angle" of drift relative to the electric field lines, and hence a compressed track pattern in one readout coordinate. But, the electron drift velocity in a liquid is low enough that the Lorentz angle effect should be negligible.

Nonetheless, in view of the novelty of operating a time projection chamber with $\mathbf{E} \perp \mathbf{B}$, we propose to study this.

1.2 Operation at High Pressure

Another issue novel to very large liquid detectors is the increase of pressure at the bottom of the tank. In principle, the drift velocity of ionization electrons is directly affected by the density of the medium, and only indirectly by the pressure to the extent that it influences the density. Since liquid argon, as with all liquids, is nearly incompressible, higher pressures should have little impact on the performance of the detector. Liquid argon has density 1.4, so the pressure increases by 1 atm for each 7 m of depth. For a LANNDD of 40 m total height, the maximum pressure is about 6 atm. We propose to verify that the electron transport in liquid argon is little affected by such pressures.

1.3 Determination of the Sign of the Electron Charge

One of the greatest advantages of a magnetized liquid argon detector is its ability to determine the sign of an electron up to a few GeV, by detailed analysis of its electromagnetic shower for which the radiation length is 14 cm. Measurement of the curvature of the electron trajectory before, and after, the first bremsstrahlung provide the signature of the electron charge, as illustrated in Fig. 3.

1.4 The μ-LANNDD Proposal

In view of electromagnetic shower fluctuations, it is important to verify the efficiency of the electron charge determination as a function of electron energy in actual experimental conditions. This requires a detector beyond the scope of the present proposal, but which is being proposed elsewhere by a collaboration including the authors [19]. For this, a liquid argon detector some $38 \times 38 \times 210$ cm^3 with horizontal drift over 38 cm will be placed inside a 1-T magnet with vertical field, as sketched in Fig. 4.
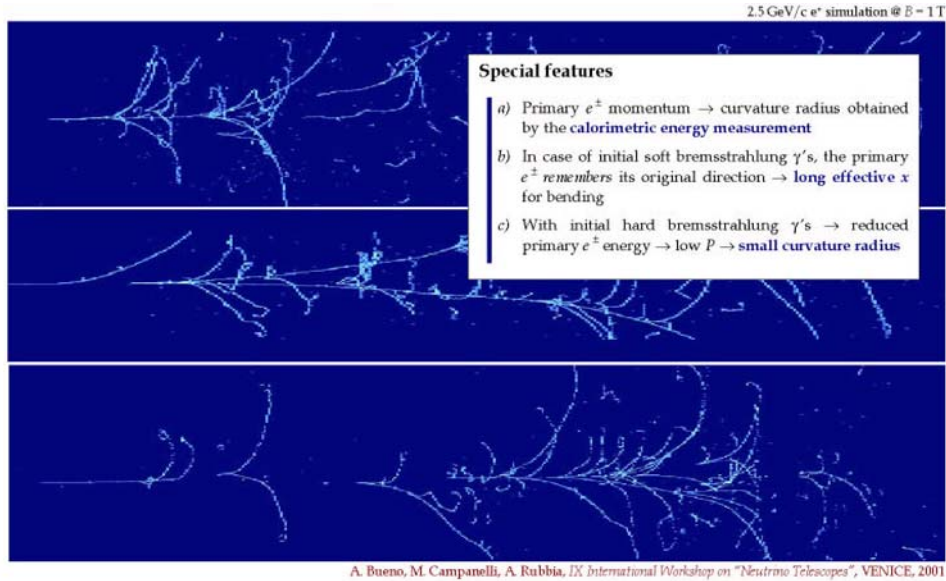
Figure 3: Simulations of electromagnetic showers of 2.5 GeV electrons in liquid argon with a 1-T transverse magnetic field [23].
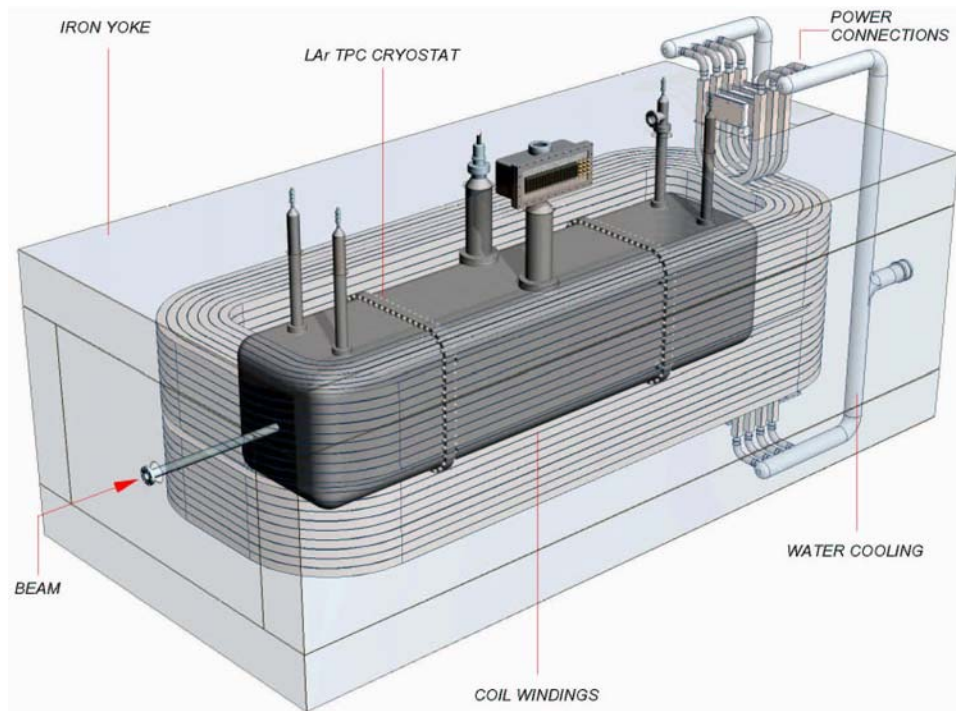

Figure 4: Sketch of the μ-LANNDD detector being proposed to study the efficiency of electron charge determination in a magnetized liquid argon detector [19].

2 The R&D Program

2.1 The Test Chamber

Two of the three major R&D goals for a magnetized liquid argon chamber can be accomplished with a small test chamber, sketched in Fig. 5, that can be placed in a magnetic field. This device, which is the heart of the present proposal, will be used to verify that good collection of ionization electrons occurs when the drift electric field is perpendicular to the magnetic field, and that good collection of electrons occurs at pressures up to 6 atmospheres. The third goal of determining the efficiency of electron charge measurement *vs.* electron energy is beyond the scope of the present proposal, and will be pursued by the authors, and others, elsewhere [19].
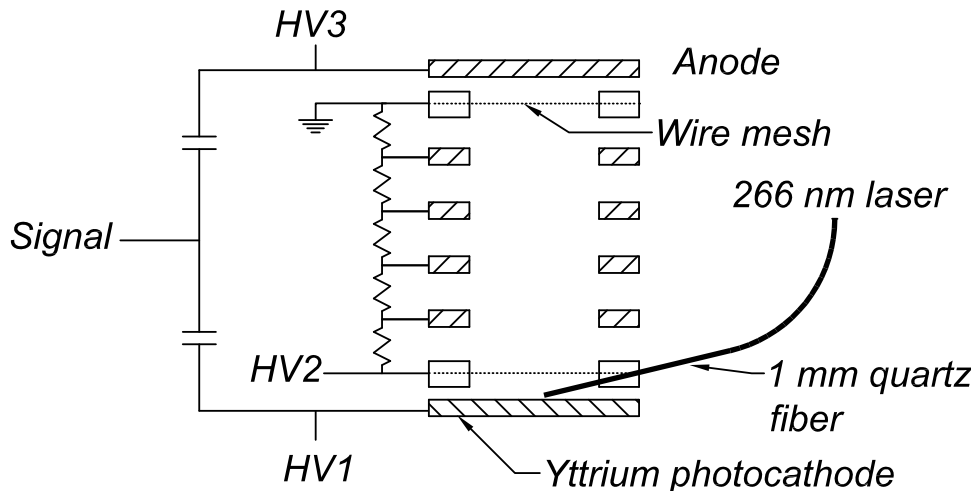

Figure 5: Sketch of the proposed test chamber. The central drift region between the two wire mesh grids is 50 mm long and 25 mm in diameter.

The test chamber is a small time projection chamber based on designs for chambers that can determine the lifetime of ionization electrons in liquids [9, 10, 11, 18].

Electrons are ejected from the cathode by the photoelectric effect of a pulse of 266 nm light. We proposed to purchase a Pulselas frequency-quadrupled, Q-switched, diode-pumped laser from Alphalas [24]. This laser can deliver up to 20kHz of pulses, each of about 1 μJ, or $\approx 6 \times 10^{12}$ UV photons. We choose a yttrium photocathode because of its relatively high quantum efficiency for an oxidized metal. Tests in our lab have shown that yttrium is superior to, for example, magnesium, which has been measured to have a quantum efficiency of 10^{-3} at 266 nm [25]. Even if the coupling of the laser pulse into the 1-mm-diameter optical fiber (with a cryogenic feedthrough [26]) is as poor as 0.01, we should still have over 10^7 photoelectrons per pulse.

The test chamber is divided into three regions in which the electric field can be separately adjusted. Two wire meshes bound the central drift region, which is surrounded by injection and collection regions. With electric fields in the injection, drift, and collections regions in the ratios of 1:4:16, electrons all pulled past the mesh with greater than 99% efficiency [8].

The cathode and anode are both connected (via blocking capacitors) to a single low-noise preamp, as shown in Fig. 5. If all electrons ejected from the photocathode arrive at the anode, the readout pulse shows an initial rise, followed by a fall back to ground after the delay time of the electrons across the chamber. If instead, the purity of the liquid is poor and electrons are attached during their drift, the fall of the pulse collected at the anode will be incomplete, as shown in Fig. 6 from [18]. The ratio of the extent of the fall to that of the rise permits a determination of the electron lifetime [9].
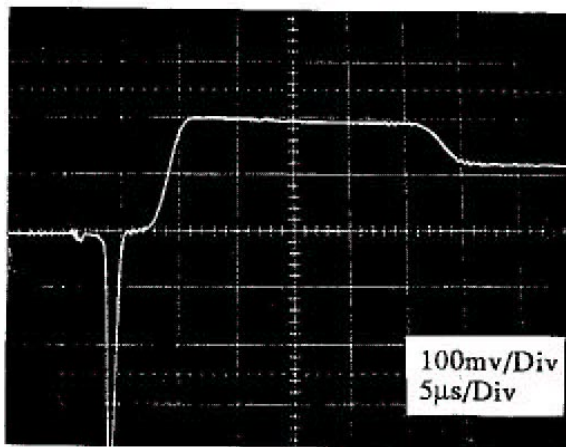

Figure 6: A typical pulse in an electron lifetime chamber [18], when the lifetime is poor.

Typically a noise pulse from interference from the Q-switched laser precedes the rise of the desired signal. It is also possible that electrons are ejected from other materials in the chamber by the part of the laser pulse reflected from the cathode, which electrons then find their way into the drift and collection regions. Should these effects prove to be troublesome, a more complex design of the injection gap can help suppress these noise sources [18].

2.2 Argon Purification

At liquid-argon temperature, the main source of electron attachment is residual oxygen. Electron attachment by oxygen in a liquid medium is more probable than in a gas, because the proximity of neighbor atoms in a liquid permits the oxygen ion to de-excite before the electron detaches [27]. A simple model consistent with the experience of the ICARUS group is that an electron drifting in liquid argon will become stuck on the first oxygen molecule it encounters – within one molecular radius of the electron's trajectory. That is, a 2-m drift path requires a purity of 0.1 ppb of oxygen, since there are 10^{10} 2-angstrom-diameter argon atoms over this length.

The experience of the ICARUS group is that this level of oxygen purity can be achieved using commercial Oxisorb cartridges [28], provided care is taken in the purification sequence. Our proposed purification system is shown in Fig. 7. Besides the test chamber and Oxisorb cartridge, a separate storage tank is used for initial purification, and for temporary storage of the purified argon should the test chamber needed to be opened briefly.
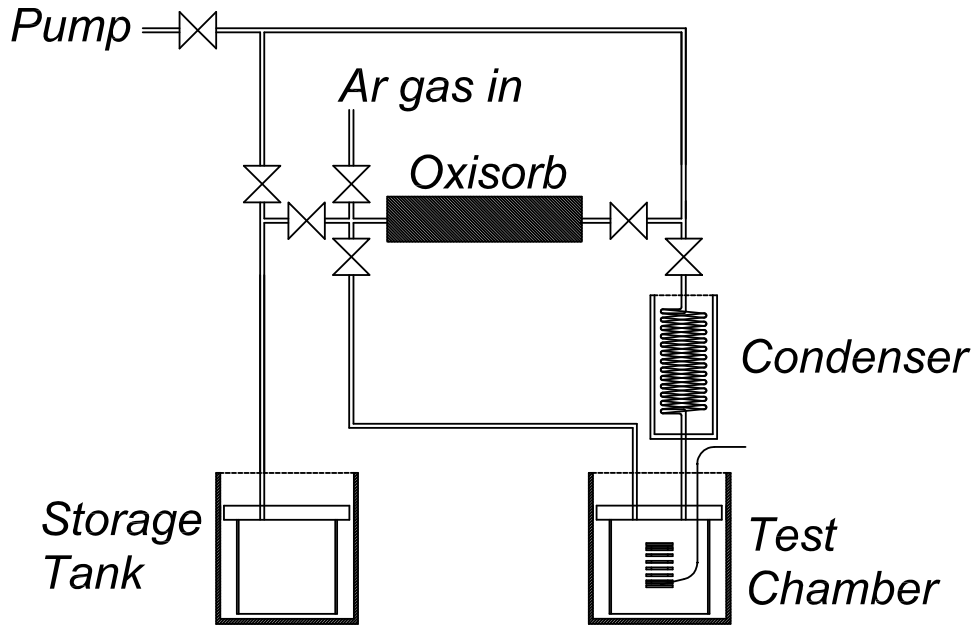
7

Figure 7: The argon purification system, based on an Oxisorb cartridge.

A single 200 ft^3 bottle of high purity argon (10-100 ppm) is sufficient for this project, since liquid argon has a volume 1/800 that of gas at STP. After the initial baking and pumpdown of the entire system, argon gas is introduced from the bottle through the Oxisorb cartridge and condensed in the storage tank, which is bathed in liquid nitrogen. The test chamber is sealed off at this stage. After the initial condensation, the Oxisorb cartridge is baked and pumped down to remove such non-oxygen contaminants as may have collected in it. Then, the storage tank is allowed to warm up, and the test chamber opened so the argon is distilled over into the test chamber, which is bathed in low-purity liquid argon.

Once the test chamber is at the desired liquid level (as measured by internal sensors [29]), the storage tank is closed, and the Oxisorb flow loop opened. The latter is driven by argon boiling off the surface of the liquid in the test chamber (which should actually not be too well insulated or the flow won't happen). To permit the loop to flow, the repurified argon gas must be condensed at the output from the Oxisorb cartridge in a separate condenser coil, also bathed in low-purity liquid argon, so that it can fall into the test chamber.[2]

2.3   Performance in a Magnetic Field

To verify the operation of a liquid argon time projection chamber in a magnetic field perpendicular to the drift electric field, we will place the test chamber in a 0.5-T C-type magnet that is open on top, as shown in Fig. 8. This magnet will be a reconfigured version of a magnet that produced a 1-T field across a 5″ gap [30]. By widening the gap to 10″ to accommodate the test chamber and its dewar, while reducing the magnetic field from 1 to 0.5 T, the magnet power consumption will remain essentially unchanged.

---

[2]Without the external condenser, there would be nothing to break the symmetry of the flow loop, and the argon wouldn't know which way to flow.

Should it prove desirable to study the chamber with **B** parallel to **E**, the chamber could be rotated by 90° and remounted within its vacuum vessel.
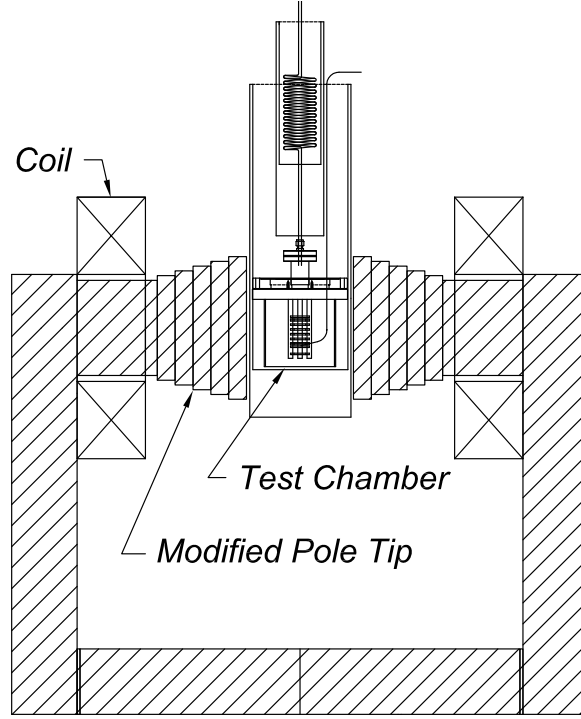

Figure 8: Sketch of the test chamber mounted in the 0.5-T magnet.

The electric field strength in the central drift region of the test chamber will be about 300 V/cm (= 1 statvolt/cm), and the corresponding electron drift velcity is about 1.3 mm/μs [14]. This is at the upper end of the linear regime of velocity *vs.* field strength, where the mean free path is only a few argon atoms,[3] and the collision time τ is about 5×10^{-13} s.

When the electron drift takes place in a magnetic field of strength B, the electron has cyclotron frequency $\omega_B = eB/mc = 1.7 \times 10^7 B$ [gauss]. Thus, for $B = 0.5$ T = 5,000 gauss, $\omega_B = 9 \times 10^{10}$/s, and the corresponding period is $\tau_B = 2\pi/\omega_B \approx 7 \times 10^{-11}$ s $\approx 0.01\tau$. That is, the collision frequency is almost 100 times the cyclotron frequency in a 0.5-T field, so we expect that the electron drift is hardly affected by such a magnetic field.

Another way of stating this result is that the Lorentz angle, $\theta = \tan^{-1} vB/cE \approx 0.03$, is small. The trajectory of the drift electrons in the test chamber will be offset by about 1.6 mm over the 50 mm central drift region. To detect this effect, we will use an anode plane segmented into 1 mm strips. To simplify the readout electronics, we will only instrument

---

[3]The drift velocity $v = \lambda/\tau$ is related to the electric field E, the mean free path λ, and the mean free time τ by,

$$v = \frac{1}{2}\frac{eE}{m}\tau = \frac{1}{2}\frac{e\hbar}{m^2c^3}\frac{mc}{\hbar}c^2E\tau = \frac{1}{2}\frac{c^2}{E_{\rm crit}\lambda_C}E\tau = \frac{1}{2}\frac{9 \times 10^{20} \text{ cm}^2/\text{s}^2}{(1.6 \times 10^{16} \text{ V/cm})(4 \times 10^{-11} \text{ cm})}E\tau \approx 8 \times 10^{14}E\tau.$$

Thus, $E = 300$ V/cm and $v = 1.3$ mm/μs $= 1.3 \times 10^5$ cm/s implies that the mean free time is $\tau \approx 5 \times 10^{-13}$ s, and the mean free path is $\lambda = v\tau \approx 8 \times 10^{-8}$ cm, *i.e.*, a few atomic diameters.

one of these strips at a time, mapping out the profile of charge collection at the anode during a series of short data runs.

2.4   Performance at 6 Atm

As noted above, the mean free path for drifting electrons in liquid argon is a few atomic diameters. Because liquid argon is nearly incompressible, we expect that the mean free path, and hence the electron mobility, is little affected by increased pressure [31]. The maximum pressure at the bottom of a 40-m-high LANNDD detector is about 6 atm, which is about the maximum pressure that can be safely sustained in the proposed test chamber (whose construction is based on components typical of the vacuum industry).

We therefore propose to pressurize the test chamber (with boiloff from the storage tank of purified argon) for short data runs to confirm the expectation that electron drift properties are largely independent of pressure.

3   Budget

We propose a budget of $30k for this R&D project.

This budget includes $10k for a Q-switched, frequency-quadrupled YAG laser, and $20k for materials and supplies. The latter include stainless-steel vacuum components, cryogenic electrical feedthroughs, piping, valves, small dewars, cryogenic liquid level meters, a mass flowmeter, yttrium metal for the cathode, an Ortec 142A low-noise preamp, a data-collection PC, Oxisorb cartridges, various hardware for mounting the detector and purification system, argon and nitrogen gas and liquid.

Technician time for the fabrication of the detector will be provided by Princeton University. The magnet and a 20-kW power supply will be reconfigured from surplus equipment in the Princeton Physics Department.

4 Biographical Sketch of Kirk T. McDonald

Date of Birth:	Oct. 20, 1945
Place of Birth:	Vallejo, California
Nationality:	USA
Marital Status:	Married, 2 children
Work Address:	Princeton University
	P.O. Box 708
	Princeton, NJ 08544
Telephone:	609-258-6608
Fax:	609-258-6360
E-mail:	mcdonald@puphep.princeton.edu
Web-site:	http://puhep1.princeton.edu/m̃cdonald/
Bibliography:	http://puhep1.princeton.edu/m̃cdonald/bib.pdf

Education:

1966-1972	Doctor of Philosophy in Physics
	Caltech
1963-1966	Bachelor of Science in Mathematics and Physics
	University of Arizona

Employment History:

Sep. 1985 –	Professor of Physics, Princeton University
Sep. 1980 – Aug. 1985	Associate Professor of Physics, Princeton University
Sep. 1976 – Aug. 1980	Assistant Professor of Physics, Princeton University
Jan. 1975 – Aug. 1976	Fermi Fellow, University of Chicago
July 1972 – Dec. 1974	Postdoctoral Fellow, CERN

Professional Organizations:

Fellow of the American Physical Society

Member of the American Association for the Advancement of Science

Member of the American Association of Physics Teachers

Member of the American Association of University Professors

Member of the Minerals, Metals and Materials Society (TMS)

Member of ASM International

References

[1] ICARUS home page: http://icarus.lngs.infn.it/

[2] D.B. Cline, F. Sergiampietri, J.G. Learned, K.T. McDonald, *LANNDD, A Massive Liquid Argon Detector for Proton Decay, Supernova and Solar Neutrino Studies, and a Neutrino Factory Detector*, astro-ph/0105442

[3] Q.V. Ahmad *et al.*. *Measurement of the Rate of $\nu_e + d \rightarrow p + p + e$ Interactions Produced by ^8B Solar Neutrinos at the Sudbury Neutrino Observatory*, Phys. Rev. Lett. **87**, 071301 (2001), arxiv.org/abs/nucl-ex/0106015, http://sno.phy.queensu.ca/

[4] C. Rubbia, *The Liquid Argon Time Projection Chamber: a New Concept for Neutrino Detector*, CERN-EP/77-08 (1977),
https://cds.cern.ch/record/117852/files/CERN-EP-INT-77-8.pdf

[5] F. Sergiampietri, *On the Possibility to Extrapolate Liquid Argon Technology to a Supermassive Detector for a Future Neutrino Factory*, presented at NuFACT'01 (May 26, 2001), http://kirkmcd.princeton.edu/nufact/sergiampietri_nufact01.pdf

[6] E. Aprile, K.L. Giboni and C. Rubbia, *A Study of Ionization Electrons Drifting Large Distances in Liquid and Solid Argon*, Nucl. Instr. and Meth. A **241**, 62 (1985),
http://kirkmcd.princeton.edu/examples/detectors/aprile_nim_a241_62_85.pdf

[7] G. Giorginis *et al.*, *A Liquid Argon TPC*, Nucl. Instr. and Meth. A **273**, 650 (1988),
http://kirkmcd.princeton.edu/examples/detectors/giorginis_nim_a273_650_88.pdf

[8] E. Buckley *et al.*, *A Study of Ionization Electrons Drifting Over Large Distances in Liquid Argon*, Nucl. Instr. and Meth. A **275**, 364 (1989),
http://kirkmcd.princeton.edu/examples/detectors/buckley_nim_a275_364_89.pdf

[9] G. Carugno *et al.*, *Electron Lifetime Detector for Liquid Argon*, Nucl. Instr. and Meth. A **292**, 580 (1990), http://kirkmcd.princeton.edu/examples/detectors/carugno_nim_a292_580_90.pdf

[10] G. Bressi *et al.*, *Argon Purification in the Liquid Phase*, Nucl. Instr. and Meth. A **292**, 585 (1990), http://kirkmcd.princeton.edu/examples/detectors/bressi_nim_a292_585_90.pdf

[11] A. Bettini *et al.*, *A study of the factors affecting the electron lifetime in ultra-pure liquid argon*, Nucl. Instr. and Meth. A **305**, 177 (1991),
http://kirkmcd.princeton.edu/examples/detectors/bettini_nim_a305_177_91.pdf

[12] P. Benetti *et al.*, *The ICARUS R&D program and results*, Nucl. Instr. and Meth. A **327**, 173 (1993), http://kirkmcd.princeton.edu/examples/detectors/benetti_nim_a327_173_93.pdf

[13] P. Benetti *et al.*, *A three-ton liquid argon time projection chamber*, Nucl. Instr. and Meth. A **332**, 395 (1993),
http://kirkmcd.princeton.edu/examples/detectors/benetti_nim_a332_395_93.pdf

[14] P. Cennini *et al.*, *Performance of a three-ton liquid argon time projection chamber*, Nucl. Instr. and Meth. A **345**, 230 (1994),
http://kirkmcd.princeton.edu/examples/detectors/cennini_nim_a345_230_94.pdf

[15] F. Arneodo *et al.*, *First observation of 140-cm drift ionizing tracks in the ICARUS liquid-argon TPC*, Nucl. Instr. and Meth. A **449**, 36 (2000),
http://kirkmcd.princeton.edu/examples/detectors/arneodo_nim_a412_440_98.pdf

[16] F. Arneodo, *Operation of a 10 m^3 ICARUS detector module*, Nucl. Instr. and Meth. A **461**, 286 (2001), http://kirkmcd.princeton.edu/examples/detectors/arneodo_nim_a461_286_01.pdf

[17] F. Arneodo *et al.*, *ICARUS:an innovative detector for underground physics*, Nucl. Instr. and Meth. A **461**, 324 (2001),
http://kirkmcd.princeton.edu/examples/detectors/arneodo_nim_a461_324_01.pdf

[18] P. Benetti *et al.*, *A simple and effective purifier for liquid xenon*, Nucl. Instr. and Meth. A **329**, 361 (1993), http://kirkmcd.princeton.edu/examples/detectors/benetti_nim_a329_361_93.pdf

[19] F. Sergiampietri *et al.*, *μ-LANNDD, A prototype magnetized liquid argon detector for electron charge sign discrimination* (Oct. 23, 2001),
http://kirkmcd.princeton.edu/nufact/uL_proposal_102301.pdf

[20] S. Ozaki *et al.*, eds., *Feasibility Study-II of a Muon-Based Neutrino Source*, (June 14, 2001), http://www.cap.bnl.gov/mumu/studyii/FS2-report.html

[21] M.V. Diwan *et al.*, *A Scenario for a Brookhaven Neutrino Super Beam Experiment*, Proc. Snowmass'01 (Oct. 23, 2001),
https://www.slac.stanford.edu/econf/C010630/papers/E103.pdf

[22] Y. Itow *et al.*, *The JHF-Kamioka neutrino project* (June 5, 2001), arxiv.org/abs/hep-ex/0106019

[23] A. Bueno, M. Campanelli and A. Rubbia, *Neutrino factories: Detector concepts*, IX Intl. Workshop on Neutrino Telescopes (Venice, Mar. 6-10, 2001),
https://arxiv.org/abs/hep-ph/0106088

[24] Alphalas GmbH, Göttingen, Germany, http://www.alphalas.com

[25] T. Srinivasan-Rau, *Magnesium Photocathode Efficiencies vs. Photon Energy Compared to Cu and Cs_2Te* (Mar. 29, 1995),
http://nslsweb.nsls.bnl.gov/AccTest/capfiles/photocat/quantum_eff.html

[26] Oz Optics LTD, Ontario, Canada K0A 1L0, http://www.ozoptics.com

[27] D.H. Swan, *Electron Attachment Processes in Liquid Argon containing Oxygen or Nitrogen Impurity*, Proc. Phys. Soc. **82**, 74 (1963),
http://kirkmcd.princeton.edu/examples/detectors/swan_pps_82_74_63.pdf

[28] In the USA, Oxisorb cartridges can be ordered from Frank Tamandl of MG Industries, Alllentown, PA, 610-530-5342, http://www.mgindustries.com/gts/SpecGasEquip/Filtration.pdf

[29] We have verified that two commercial liquid-nitrogen level sensors also function correctly with liquid argon: Model LN2-1000 from Key High Vacuum Products, http://www.keyhigh.com/ and Model 250 from Cryomagnetics, http://www.cryomagnetics.com/

[30] H. Bichsel, R.F. Mozley and W.A. Aron, *Range of 6- to 18-MeV Protons in Be, Al, Cu, Ag, and Au*, Phys. Rev. **105**, 1788 (1957), http://kirkmcd.princeton.edu/examples/detectors/bichsel_pr_105_1788_57.pdf

[31] H. Schnyders, S.A. Rice and L. Meyer, *Electron Mobilities in Liquid Argon*, Phys. Rev. Lett. **15**, 187 (1965), http://kirkmcd.princeton.edu/examples/detectors/schnyders_prl_15_187_65.pdf